Medium-scale Laboratory Model of Mono-bucket Foundation for Installation Tests in Sand

Koteras, Aleksandra Katarzyna; Ibsen, Lars Bo

Published in:
Canadian Geotechnical Journal

DOI (link to publication from Publisher):
10.1139/cgj-2018-0134

Publication date:
2019

Document Version
Early version, also known as pre-print

(i) Title of paper:

Medium-scale Laboratory Model of Mono-bucket Foundation for Installation Tests in Sand

(ii) Authors:

1. Aleksandra Katarzyna Koteras
2. Lars Bo Ibsen

(iii) Affilation and address for each author:

1. Ph.D. student, Department of Civil Engineering, Aalborg University, Aalborg, Denmark, akl@civil.aau.dk
2. Professor, Department of Civil Engineering, Aalborg University, Aalborg, Denmark, lbi@civil.aau.dk

(iv) Aleksandra Katarzyna Koteras, Ph.D. Student, Department of Civil Engineering, Aalborg University, Thomas Manns Vej 23, 9220 Aalborg Ø, Denmark, Phone: +4591470101, Email: akl@civil.aau.dk

Abstract

This paper described medium scale test results for bucket foundation installation. The campaign includes both, the jacking and the suction installation tests in the sand. Results allow for better understanding of the interaction between the soil and the bucket skirt. Such observations are desired as there are many issues concerning the suction installation. The suction applied under the bucket lid results in seepage flow inside the surrounding sand. The seepage flow plays a pivotal role in the reduction of the penetration resistance and, therefore, allows for the full penetration despite of the initial large soil resistance. On the other hand, the loosening of inside soil plug might become problematic when the soil approaches its failure stage. The failure happens as a result of soil piping or due to extensive soil heave inside the bucket foundation. All aspects are still not fully understood and challenging, while capturing them into the design, therefore, they are addressed in this paper. Additionally, measurements of pore pressures around the bucket skirts are compared with results of numerical simulations. This allows for validation of the FE-model and enables the analysis of the soil behavior around the skirt.

Keywords: Bucket foundation, Dense sand, Suction, Seepage, Soil resistance

Introduction

The development in offshore wind energy comes together with the increase in research, where the main purpose is seen in the reduction of the total cost of wind turbines. Budget cuts can be found in the design of the foundation; therefore, new, more cost-effective solutions are desirable. Such a solution is seen in the suction bucket foundation technology, where the bucket lid is equipped with special valves allowing for suction installation. This is a great advantage over the jacking installation. The suction process is more cost-effective and feasible, as no heavy drilling equipment is required. This makes the solution also environmental-friendly. Until today, the suction anchors have been extensively installed in various types of offshore engineering devices and systems across different offshore sites. There are also well-documented examples of skirted structures installed as foundations (Tjelta 1995, Andersen et al. 2008). The suction bucket foundation for a wind turbine was used in Frederikshavn, Denmark. The 5-year research project documenting installation and operation of the wind turbine is described by Ibsen (2008).

The area of focus for a number of offshore projects takes place in the North Sea, where the seabed consists mainly of dense sand. In comparison with clay, the penetration resistance of cohesionless soils is much higher and the installation might seem more problematic. However, past research has shown that the suction application not only creates the downward force required for installation, but also provides a large decrease in resistance for all permeable soils. The seepage flow generated around the bucket skirt induces upward hydraulic gradient within the inner soil and downward gradient on the outside of skirt. The effective soil stress is therefore changed, but overall resulting in reduction of the total soil penetration resistance. Many studies on the installation of suction bucket foundation in sand have been published, proposing different calculation methods for the installation process (Erbrich and Tjelta 1999, Houlsby and Byrne 2005, Andersen et al. 2008, Senders

and Randolph 2009). However, these methods show only the reduction in soil resistance based on the value of applied suction without even analyzing the interaction between the bucket skirt and the surrounding soil during the seepage flow.

The installation process for suction bucket foundation in sand consists of two parts: the self-weight penetration and the suction penetration. The first stage is necessary in order to create a sufficient seal between the skirt of the bucket and the surrounding soil without which the suction application is not effective. In the second phase of the installation, the required suction for given penetration depth must be designed for. Whereas this general principle is known, improvements on the detailed design for the installation are still required. The paper presents medium-scale tests for the bucket foundation installation by the use of two different methods: jacking and suction installation. The pore pressures around the bucket skirt and the applied suction under the bucket lid are monitored during the installation tests. The model during the installation is presented in Fig.1. The analysis of the measurements re-confirms the known-findings about the reduction in soil resistance, but it also allows for thorough investigation of the seepage flow around the bucket foundation. In addition, the paper contains results of numerical simulations that represent the suction installation tests with the same conditions as the set-up in the laboratory. The comparison of both results allows the analysis of the critical allowable suction for the bucket foundation installation and better understanding of experimental results.

Figure 1. Installation of the bucket model in the sand container

Soil penetration resistance of skirt structures

Calculation Methods

The calculation of penetration resistance can be either based on the ultimate bearing capacity theory or on the empirical model that relates the results of the CPT to the soil penetration resistance. In general, the total penetration resistance, R_{tot}, consists of the skirt tip resistance, Q_{tip}, and inner and outer friction along the skirt, F_{inner} and F_{outer} respectively. Eq. (1) presents the classical approach based on the bearing capacity theory for the pile design (API 2014).

$$\mathrm{R_{tot}} = \mathrm{A_{tip}} \cdot min\left[\sigma'_{\mathrm{v}}(\mathrm{h}) \cdot \mathrm{N_q}, \mathrm{Q_{lim}}\right] + \left(\mathrm{A_{s,o}} + \mathrm{A_{s,i}}\right) \cdot min\left[\mathrm{K} \cdot \tan\delta \cdot \int_0^{\mathrm{h}} \sigma_{\mathrm{v}}{}' (\mathrm{z})\mathrm{dz}, \mathrm{f_{lim}}\right], \quad (1)$$

where A_{tip}, $A_{s,o}$ and $A_{s,i}$ is the tip area, the outside skirt area and the inside skirt area respectively, σ'_v is the effective vertical soil stress, z is the depth below soil surface and h is the penetration depth. D_o and D_i are the outside and inside diameter of the bucket and Q_{lim} and f_{lim} are the suggested limit values for the tip resistance and for the skirt friction. The total resistance calculated with this

approach brings out difficulties in the estimation of soil parameters: the bearing capacity factor, N_q, the coefficient of lateral earth pressure, K, and the interface angle, δ. Therefore, the CPT-based approach seems more straightforward and accurate (DNV, 1992). As the cone from CPT device resembles the skirted foundation, results of measured cone resistance, $\mathrm{q_c}$, can be directly related to the skirt and the tip resistance of the foundation (eq. 2). The method appears to be more reliable because the CPT gives a constant record of the resistance throughout the depth. Senders et al. (2009) and Chen et al. (2016) suggest the same and show in their research that the calculated resistance based on the classical approach does not fit well within experimental data.

$$\mathrm{R_{tot}} = \mathrm{A_{tip}} \cdot \mathrm{q_c(h)} \cdot \mathrm{k_p} + (\mathrm{A_{s,o}} + \mathrm{A_{s,i}}) \cdot \int_0^{\mathrm{h}} \mathrm{q_c(z)dz} \cdot \mathrm{k_f} \quad (2)$$

Empirical coefficients k_p and k_f relate the cone resistance of CPT to the skirt tip resistance and the friction along the skirt respectively. A wide range of those parameters for sand are given by DNV (1992), however, many past studies on the penetration of skirted foundations have attempted to reduce this range (Lian et al. 2004, Lehance et al. 2005 and Andersen et al. 2008).

To enable detailed design of the suction installation process, the effects of seepage must be included. The applied suction, p, and the developed excess pore pressure, u, around the bucket skirt change the resistance of sand. However, the complexity of the stress state makes it difficult to provide a good estimation of those changes. According to Houlsby and Byrne (2005), the stress state used for the calculation of soil penetration resistance should be changed due to the hydraulic gradient,i, that develops in the surrounding soil. The method presented in their paper assumes that the distribution of the excess pore pressure on the inside and outside part of the skirt is linear with depth. Therefore, the applied pressure and the development of the excess pore pressure at the tip are sufficient to obtain the stress level for each penetration depth. The ratio of the excess pore

pressure at the tip of skirt to the applied suction is called the pore pressure factor, α. Houlsby and Byrne (2005) proposed a solution for α based on numerical analyses for a uniform hydraulic conductivity (eq.3) and for a different hydraulic conductivity of the inside plug (eq.4). The ratio between inside and outside hydraulic conductivity, k_i and k_o respectively, is termed as k_{ratio}.

$$\alpha_1 = 0.45 - 0.36 \cdot \left(1 - exp\left(-\frac{\mathrm{h}}{0.48 \cdot \mathrm{D}}\right)\right) \quad (3)$$

$$\alpha = \frac{\alpha_1 \cdot k_{ratio}}{(1-\alpha_1) + \alpha \cdot k_{ratio}} \quad (4)$$

The reduced soil resistance is calculated by replacing the effective soil unit,γ',with its reduced or increased value for upward gradient on the inside skirt and for the downward gradient on the outside skirt respectively $\left(\gamma' - \frac{(1-\alpha)\cdot p}{h};\ \gamma' + \frac{\alpha \cdot p}{h}\right)$. The comparison of the calculated resistance with the installation cases showed a good fit. However, key soil parameters where optimized to get such a fit and to get a precise calculation of the resistance, a lot of experience with this method is still required.

Koteras et al. (2016) proposed another formulation that gives the best fit to the results of numerical analysis performed in PLAXIS 2D. Eq.(5) is found for the installation in sand of uniform hydraulic conductivity.

$$\alpha = \frac{0.21}{\frac{\mathrm{h}}{\mathrm{D}} + 0.44} \quad (5)$$

Critical pressure for suction installation

The design method for suction installation must comply with any possible limitations. One of those is the critical pressure, p_{crit}, that can be applied under the bucket lid during the installation. As the hydraulic gradient appears inside the surrounding soil, the sand on the upward flow side becomes

looser. At some stage, the decrease in soil density can cause the complete loosening of soil around the skirt and as a result, the seal between the bucket skirt and the soil is broken. The installation process cannot proceed due to loss of seal and such a state is denoted as piping. The hydraulic gradient causing a drop of effective soil stress to zero is called the critical gradient, $i_{crit} = \frac{\gamma'}{\gamma_w}$. Even though, as first, the critical hydraulic gradient is achieved around the tip of the skirt, the localized pipes are constrained with surrounding soil. The critical gradient then proceeds upward, along the skirt, until it reaches the inner soil surface. The hydraulic gradient controlling the piping is the exit gradient that appears at the inner soil surface adjacent to the skirt (Senders and Randolph 2009). Critical pressure studies are normally performed with numerical simulations.

Erbrich and Tjelta (1999) proposed a solution for a critical suction number, S_N, that shows the applied suction that causes the critical hydraulic gradient as a function of penetration ratio, $\left(\frac{h}{D}\right)$. The penetration depth is denoted as h, and the diameter of foundation as D. The solution is based on steady-state flow calculations performed numerically. More recent studies relate the critical suction to a value of normalized seepage length, $\left(\frac{s}{h}\right)$. The seepage length, s, is expressed from the definition of the hydraulic gradient at the exit, i_{exit}, which is calculated by dividing the change of hydraulic head, ΔH, by the seepage length. Then the seepage length can be calculated as:

$$\mathrm{s} = \frac{\mathrm{p}}{\mathrm{i_{exit}} \cdot \gamma_\mathrm{w}} \tag{6}$$

Senders and Randolph (2009) performed numerical simulations in PLAXIS. To obtain a normalized seepage length as a function of penetration ratio results of PLAXIS are analyzed together with results published by Erbrich and Tjelta (1999) and the theoretical values for a sheet-pile wall.

148 $$\left(\frac{s}{h}\right)_{exit} = \pi - atan\left[5 \cdot \left(\frac{h}{D}\right)^{0.85}\right] \cdot \left(2 - \frac{2}{\pi}\right) \quad (7)$$

149 The critical pressure against piping is calculated by combining equations for the critical gradient and
150 for the seepage length (eq.8).

151 $$\frac{p_{crit}}{\gamma' \cdot D} = \left(\frac{h}{D}\right) \cdot \left(\frac{s}{h}\right) \quad (8)$$

152 It is assumed that: the inner friction along the skirt and the skirt tip resistance decrease linearly from
153 its maximum value, when no suction is applied, to zero, when the critical suction is achieved; the
154 outside friction along the skirt is unaffected (Senders and Randolph 2009). The reduced soil
155 resistance is calculated with eq.(9) and it is valid for $p \leq p_{crit}$.

156 $$R_{reduced} = \left(Q_{tip} + F_{inner}\right) \cdot \left(1 - \frac{p}{p_{crit}}\right) + F_{outer} \quad (9)$$

157 The proposed method gives a good fit with results of suction installation tests performed in
158 centrifuge. However, when comparing to the installation field tests, the critical suction is exceeded
159 with no failure occurrence.

160 A similar solution based on simulations performed in FLAC is presented in (Ibsen and Thilsted, 2010).
161 Eq.(10) was found to fit data best. However, the applied suction during the installation tests in
162 Frederikshavn (Denmark) exceeded the calculated critical suction and the explanation for that is
163 found throughout the empirical expression for the normalized seepage length of the case where a
164 flow boundary is situated below the sand. The flow boundary can be for example a thin less
165 permeable layer, and its presence increases the critical suction.

166 $$\left(\frac{s}{h}\right)_{exit} = 2.86 - atan\left[4.1 \cdot \left(\frac{h}{D}\right)^{0.74}\right] \cdot \left(2 - \frac{1.8}{\pi}\right) \quad (10)$$

Koteras et al. (2016) conducted also a similar study in PLAXIS 2D. Eq. (11) was given for normalized seepage length for exit hydraulic gradient. The CPT-based method is used for calculation of soil resistance during the installation. However, the changes in outside and inside friction on the skirt and the change in skirt tip resistance are based on normalized seepage lengths obtained for hydraulic gradients calculated on the inside skirt, outside skirt and around the skirt tip respectively. A comparison with laboratory or field tests has not yet been made.

$$\left(\frac{\mathrm{s}}{\mathrm{h}}\right)_{\mathrm{exit}} = \pi - atan\left[3.6 \cdot \left(\frac{\mathrm{h}}{\mathrm{D}}\right)^{0.74}\right] \cdot \left(2 - \frac{1.8}{\pi}\right) \tag{11}$$

Lian et al. (2014) and Chen et al. (2016) conducted laboratory tests on the suction installation of bucket foundation in sand. A medium-scale model of the bucket with a diameter of 0.5m and a skirt length of 0.5m was used in the former research and a large-scale model of the bucket with a diameter of 1.5m and a skirt length of 0.5m in the latter research was used. Those models were equipped with soil pressure tensors in order to record the soil resistance on the inside and outside of the skirt. The suction measured during the installation in both cases exceeded the critical value based on (Senders and Randolph, 2009).

Lian et al. (2014) proposed the reduction coefficients for the inside friction on the skirt and for the tip resistance. The outside skirt friction is not affected. When the suction falls below the critical value, the reduction is linear between the maximum soil resistance and the zero value. However, as the critical suction was exceeded without any failure, the range for applied pressure is increased by factor 1.5. For the suction between the range of p_{crit} to $1.5p_{crit}$, there is no resistance from the outside skirt and from the tip.

Chen et al. (2016) concluded on their test results that the change in resistance is not linear and it is also different between the inner skirt friction and the tip resistance. The outside skirt friction is again not affected. Therefore, the reduction ratios, β_I and β_{tip}, were presented (eq.12 and eq.13) and it is proposed to calculate the soil penetration resistance as showed in eq.(14).

$$\beta_I = 0.865 \cdot \left(\frac{p}{p_{crit}}\right)^{1.03} \quad (12)$$

$$\beta_{tip} = 0.707 \cdot \left(\frac{p}{p_{crit}}\right)^{1.86} \quad (13)$$

$$R_{reduced} = Q_{tip}(1 - \beta_{tip}) + F_{inner}(1 - \beta_I) + F_{outer} \quad (14)$$

Summing up, either the theory based on bearing capacity, or the CPT-based approach is used for the calculation of soil penetration resistance during bucket foundation installation, the effects of suction-induced seepage must be accounted. Presented methods lack accuracy as they assume linear changes of soil resistance with penetration depth. Only Chen et al. (2016) proposed that those changes are non-linear. To analyze the soil stress changes during suction installation, medium or large scale tests are required in order to detect an interaction between the soil and the bucket skirt. As the change that really happens during the suction installation it is the development of the excess pore pressure around the bucket skirt, it seems the most adequate to record the excess pore pressure during tests. Therefore, the study presented in this paper focuses on these records.

Loosening of soil plug

For the suction installation, the seepage induced inside the soil reduces the inside soil resistance This might result in the change of the soil hydraulic conductivity inside the bucket. Houlsby and Byrne (2005) reported that reasonable fits of calculated resistance with field tests are obtained when applying the pore pressure factor for increased k_{in}. The comparison of the reduction in soil

208 resistance with centrifuge results presented by Tran and Randolph (2008) gives much better fit for
209 the case where $k_{ratio}$is equal to 1.5. Harireche et al. (2014) have shown results of the numerical
210 analysis for pressure gradient development inside the soil related to the change in soil resistance.
211 The comparison with centrifuge tests results presented by Tran and Randolph (2008) shows that
212 k_{ratio}should not only be bigger than unity but also should increase for increasing penetration depth.
213 Whether the hydraulic conductivity inside the bucket should be increased and how exactly it should
214 be included into the design method is still unclear and requires the further experience.

215 **Laboratory Model and Test Procedure**

216 ***Set-up and bucket foundation model***

217 The main aim of the laboratory tests is to analyze the soil-skirt interaction during installation of
218 bucket foundation model. The set-up is shown in Fig. 2. Vaitkunaite et al. (2014) first introduced this
219 facility for testing bucket foundation capacity in sand. After adjustments, the same set-up is used
220 for testing the installation procedure of bucket foundation, including both the jacking installation
221 and the installation due to the applied suction.

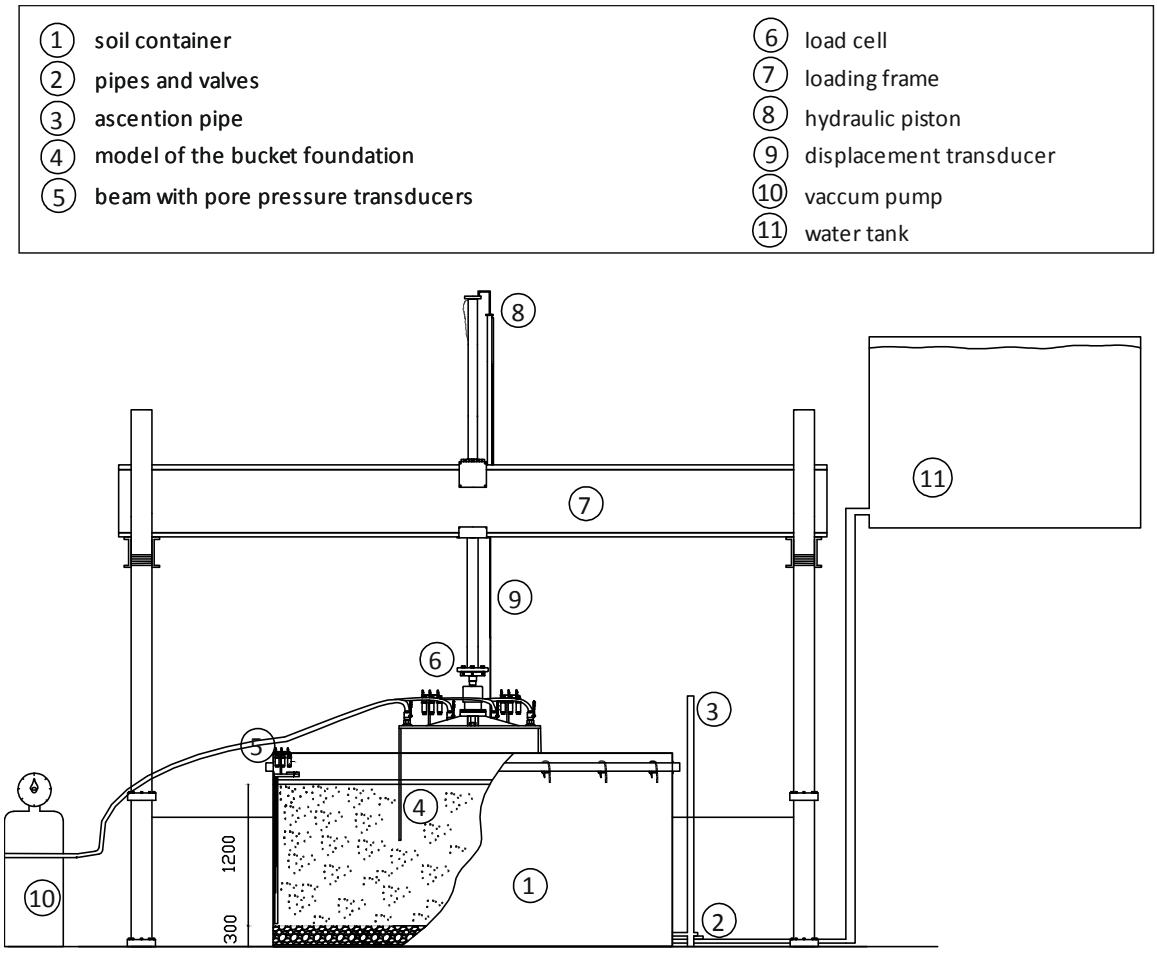

Figure 2. Laboratory set-up (dimensions in mm)

A soil container is equipped with a drainage system that consists of pipes equally distributed over the bottom, a 30 cm layer of highly permeable gravel, a geotextile sheet for prevention of sand particles to move downwards and a 1.20 m layer of sand with properties described in the following section. The internal diameter of the soil container is equal to 2.5m and the height of the container is equal to 1.52m.

The model of the bucket foundation (Fig. 3) is in a medium-scale, corresponding to a prototype size in scale 1:10. The diameter, D, is 1 m and the skirt length, d, is 0.5 m. The thickness of skirt, t, is

equal to 3 mm. The self-weight of the model, including the connection flange to the loading system, is 201kg. The bucket model is equipped with 4 valves situated on the lid that are connected to the vacuum system during the suction procedure. 6 pore pressure transducers are attached to the bucket skirt and under the bucket lid. These allow for a continuous analysis of the seepage flow around the skirt during installation. Pressure is measured through the open ended pipes attached to the skirt. The open ends are positioned at PP1-PP3 on the outside skirt and at PP4-PP6 on the inside skirt and under the bucket lid. The displacement transducer is attached to the top of bucket model and it measures a continuous record of its displacement during tests. Additionally, a beam with pore pressure transducers installed close to the edge of soil container allows the control of the boundary conditions.

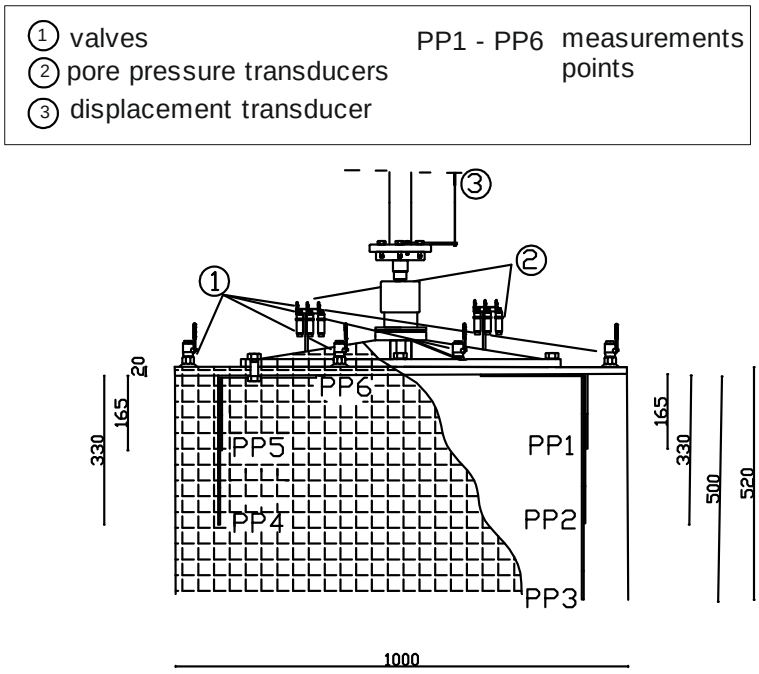

Figure 3. Model of bucket foundation (dimensions in mm)

Soil material

The chosen soil material is the Aalborg University Sand no.1 that mainly contains quartz. The sand is graded; the largest grains are of round shapes and the small grains are sharp-edged. Properties were measured by Ibsen and Brødker (1994): maximum void ratio, $e_{max} = 0.854$, minimum void ratio, $e_{min} = 0.549$, 50%-quantile, $d_{50} = 0.14$ mm, uniformity coefficient, $C_u = 1.78$ and specific grain density, $d_s = 2.64$ g/cm^3. Based on CPT results important soil parameters can be derived (Ibsen et al. 2009). Those parameters are relative soil density, I_D, triaxial friction angle, φ_{tr}, triaxial dilation angle, ψ_{tr}, in situ void ratio, e_{insitu} and effective soil unit weight, γ'. The range of values from all performed tests are included in Table 1.

The soil hydraulic conductivity, k, has been assessed by falling head test for different relative densities of material (Sjelmo 2012). For dense sand of around 90% of relative soil density, test results indicate the hydraulic conductivity of around $7 \cdot 10^{-5}$ m/s.

Test Procedure

The sand is saturated during the preparation and the installation test through the drainage system. Prior to each test the sand is prepared to a dense, uniform condition. The range of relative density from all tests is 87.8% - 91.1%. Firstly, an upward hydraulic gradient of 0.9 is applied. It is controlled by valves and ascensions pipe connected to the bottom of the sand container. Next, the sand is vibrated to the desired density. A wooden plate with holes located evenly is installed on the sand container. Next, a rod vibrator is slowly pushed into the sand through every second hole, and then in the rest of the holes on the way back. Each time the vibrator is slowly pulled. The sand conditions are analyzed through the CPT before and immediately after each of the installation tests, so that the changes in soil resistance can be captured. A laboratory CPT device developed at Aalborg

University is used. The device has the cone of 15mm diameter with a cone angle of 30° and it is calibrated at the laboratory. Before the bucket installation, CPTs are performed in 4 positions, and after installation in 8 positions; 4 of them are inside the bucket, and the other 4 are situated outside, see Fig. 4. The CPTs inside the bucket are possible through the valves' holes situated on the bucket model. The CPTs after bucket installation are performed within 5 minutes after the installation process is completed. The differences in relative soil density before and after installation indicate whether there are any changes in soil density as an effect of the installation process.

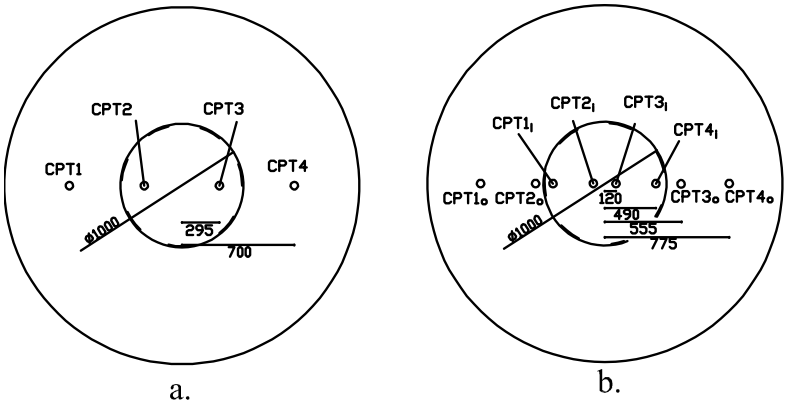

Figure 4. Positions for CPTs before (a.) and after installation test (b.) (dimensions in mm)

During the jacking installation the hydraulic piston is used to apply the required jacking force. The hydraulic motor works as a displacement control with a displacement rate of around 0.13 mm/s. The valves on the bucket lid are opened during installation and therefore, no excess pore pressure inside the bucket is expected. For the suction installation the process is divided into two steps, the self-weight installation and the suction application. The self-weight installation is performed by using the hydraulic motor that is switched to work as a force control. The force corresponding to the self-weight of the bucket model is applied. The achieved penetration depth provides an appropriate hydraulic seal between the soil and the bucket skirt for further suction application,

283 minimum 50 mm. Suction is then applied through the vacuum system by connecting the valves
284 situated on the bucket lid with the vacuum pump. The pressure is controlled manually on the
285 vacuum tank by increasing it slightly until penetration occurs. The level of water in the container is
286 controlled and refilled constantly, as the water is sucked by the pump during installation. Tilting of
287 the bucket model is negligible. During the installation process readings from the displacement
288 transducer, the pore pressure transducers and the force transducer are recorded. All sensors are
289 connected to the signal transducers boxes and then through the signal amplifiers called 'Spider8'
290 and 'MGC Plus', the records are transmitted to the program 'Catman' installed on the computer.
291 Koteras (2017) described more details on the model and the test procedure.

292 An overview of all tests can be found in Table 2. First three tests are suction installation tests, where
293 additional constant force of 2.01 kN was applied. This force is added to the resulting force from
294 applied suction throughout the entire penetration depth. Tests no. 04, 05 and 09 are pure suction
295 installation tests. The hydraulic motor was working as a force controlled, however, the force was
296 set to be 0 kN. The different self-weight penetration was obtained due to this procedure and its
297 effect on the results is assessed later on in this paper. Tests no. 07, 09 and 10 are jacking installation
298 tests. There are two values of maximum penetration given in Table 2. The first one is the value
299 corresponding to the maximum force recorded, also given in the table. It is the first point where the
300 bucket lid becomes in the contact with the soil. Later on the sand is still pushed and the particles
301 are re-arranged to be more equally distributed under the bucket lid. The force is then significantly
302 increased and the penetration still proceeds (second given value).

Development of hydraulic gradients

Seepage problem formulated with numerical model

The seepage problem in sand is formulated with a numerical model. Simulations on seepage flow around the bucket skirt during the installation are performed in 2D numerical program. An axisymmetric model is generated where the skirt of the bucket is simulated by using a rigid line segment with impermeable interface. This line segment has a length equal to the designed penetration depth, h, and it is situated 0.5 m from the center axis, the same distance as the radius, r, of the bucket model. The boundary at the center axis is closed for the flow. The bottom boundary and the side boundary are also modelled as closed for the flow. The total dimensions of the model are the same as the sand container's in the laboratory's set-up. The sketch of meshed model with dimensions is presented in Fig. 5.

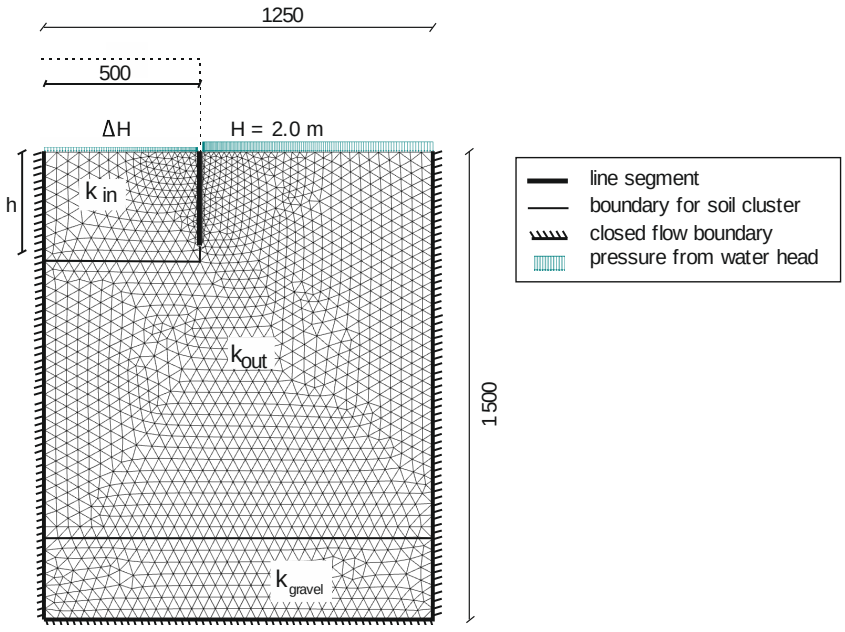

Figure 5. Meshed numerical model with boundary conditions (dimensions in mm)

316 The simulations are performed for penetration ratio, $\left(\frac{h}{D}\right)$, between 0.1 to 0.5 with interval of 0.02.
317 The continuous process of installation is here presented as a series of discrete steps, where for each
318 step the equilibrium between the soil resistance and the driving force is assumed. For each of the
319 simulation a steady-state groundwater flow calculation type is used as the seepage is approximately
320 stationary. Tran and Randolph (2008) used the same approach what gave a good agreement of their
321 numerical simulations with pressure results from centrifuge tests while installing the bucket
322 foundation. The flow around the skirt is simulated by applying flow boundary condition on the inner
323 soil surface with appropriate hydraulic head, H. The hydraulic head on the outer soil surface is
324 designed to be 2m, however, it is a random number and it should only be sufficient for a required
325 head difference, ΔH, so that a hydraulic head on the inner soil surface is not below 0. The head
326 difference is directly related to the value of the applied suction. The same model assumptions have
327 been used in (Koteras et al. 2016); however, different distances to the boundaries are applied here.

328 Suction values for each step of the numerical simulations are based on mean values from laboratory
329 test no.05 and no.09 as in those two tests the self-weight penetration of the bucket is the shortest,
330 hence the penetration due to the suction is the longest one.

331 The soil property relevant for flow calculation is a hydraulic conductivity, k. Sjelmo (2012)
332 performed a falling head tests for Aalborg University Sand no. 1 of different relative soil density. For
333 $I_D = 90.8\,\%$ a value of $k = 0.7 \cdot 10^{-4}$ m/s is proposed, whereas for $I_D = 60.5\,\%$ a value of $k = 1 \cdot$
334 10^{-4} m/s should be used. Those two values are the two closest value that are chosen to represent
335 the conditions inside the bucket skirt before and after the suction installation test. A value of $k = 1$
336 m/s is used for gravel located below the sand.

Test results

Reduction in soil penetration resistance

Results of CPT-s are investigated and relative soil density is derived based on the past CPT calibration. Fig. 6 shows a comparison of relative soil density for suction installation and for jacking installation from CPTs performed before and immediately after installation. The graph indicates the calculated relative soil density for locations inside and outside of the bucket.

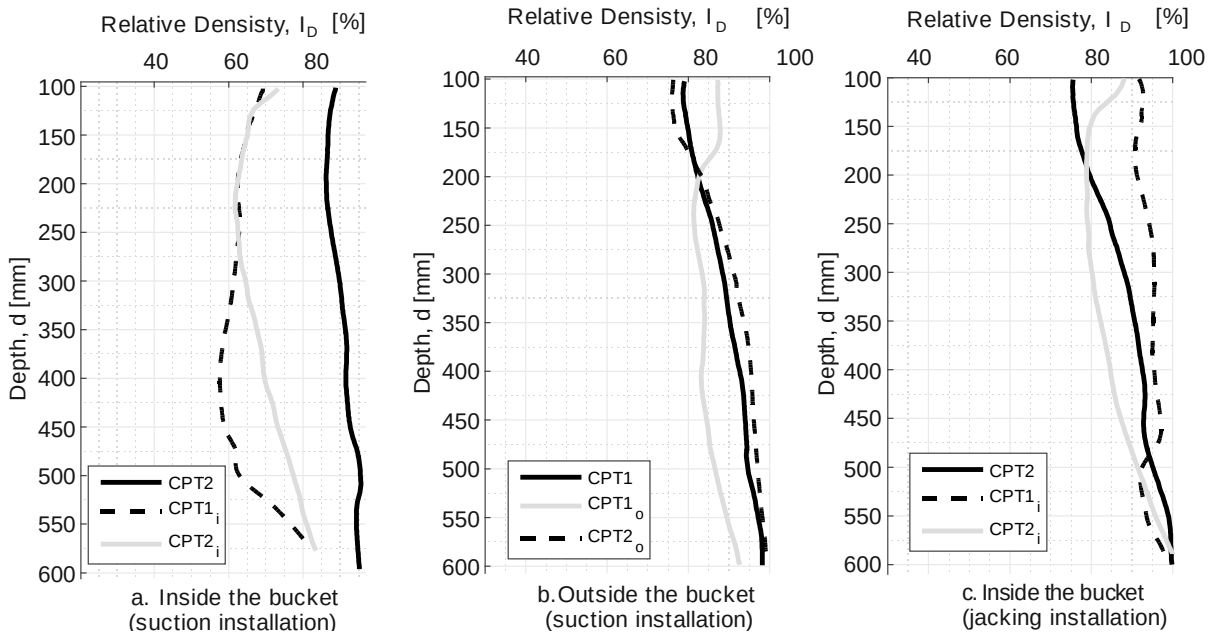

Figure 6. Comparison of relative soil density before and after installation: test no.05 (a. and b.) and test no.06 (c.); see Fig. 4 for locations of CPTs

It can be concluded that due to the suction installation and induced seepage, there is a significant decrease in soil relative density for the soil plug, whereas the changes in relative soil density on the outside of the bucket are insignificant. Results obtained after jacking installation indicates nor significant changes in relative soil density within soil plug, neither in the soil situated outside the bucket. The trend for all tests where suction installation has been performed is similar to the given example of test no.05. For all jacking installation tests, the results of CPT-s are also comparable to

352 the results of test no.06. After all jacking installation tests it was concluded that there are no
353 substantial changes in soil relative density.

354 Table 3 presents the mean values of relative soil density for each test before installation and after
355 installation; for inside soil plug and for soil outside the bucket. The upper 100 mm of sand is not
356 considered in the calculations of mean values as the results show some fluctuation resulting from
357 the presence of the sand surface. Table 3 also includes the percentage change between results
358 before and after installation, $\Delta I_{D,mean}$, for inside plug and for the soil located outside. The results
359 of relative soil density obtained before installation are compared with the results obtained after
360 installations in the two closest CPT locations (see Fig.4 for CPT locations). The mean value of the two
361 comparisons inside the bucket and of the two comparisons outside the bucket are given in the table.
362 A significant decrease in the relative soil density for inside soil plug after the suction installation is
363 observed, reaching almost to 30%. On the other hand, the changes in soil inner plug after jacking
364 installation are insignificant with a value less than 6%. For the outside soil the changes are less
365 significant and do not indicate an increase in soil resistance neither after suction nor after force
366 installation. Only values from first two tests shows a significant change of around 15%, however, in
367 both tests only locations $CPT1_o$ and $CPT2_o$ are analyzed as the signals for locations $CPT3_o$ and $CPT4_o$
368 was not recorded. Therefore, conclusions on the change in relative soil density outside the bucket
369 should not be based on those two tests. The reduction in soil relative density is directly related to
370 the reduction of soil penetration resistance. When the sand becomes looser, it resists less to the
371 skirt penetrated into the soil. This is beneficial for the installation. However, it might also lead to
372 failure and heave development.

373 Not only the reduction in soil resistance is clearly visible from CPT tests, but also when comparing
374 the force required for installation during two different installation procedures. In four tests of
375 jacking installations the results of applied force versus penetration depth are similar, as it was
376 expected due to the same soil conditions achieved before each of those tests (Fig. 7a). Mean
377 maximum value of force from all of those tests is 57 kN. The reading for the maximum value is
378 consider as the point where the displacement curve changes its pattern and becomes more flat. In
379 this point the bucket lid becomes in contact with sand. To investigate the change in required force
380 between two types of installation, the average reduction in force for suction installation, ΔF_{avg}, is
381 calculated. The average values of force from all 4 jacking tests are found for all recorded penetration
382 depths, $F_{jacking,mean}$, and compared to the force used during each of suction installations also on
383 each recorded penetration depth, $F_{suciton}$. ΔF_{avg} is then a mean value of changes in force for all
384 recorded penetration depths between 100mm to the maximum penetration depth (the depth at
385 which the lid becomes in contact with soil). For each of suction installation tests the force includes
386 the part resulting from the suction and the part resulting from the self-weight of the bucket. For
387 first three tests (01 to 03) the force includes also the additional load from hydraulic motor which
388 was used in order to investigate the different length of self-penetration to the final results. For first
389 three tests (01 to 03), the values are as follows: 43.4%, 44.8% and 46.1%. Reduction in pure suction
390 tests is slightly larger and it is equal to 56.5%, 53.8% and 49.8% for test 04, 05 and 09 respectively.
391 As an example, the average reduction in force for test no.05 is shown in Fig.7b. Based on results it
392 can be concluded that there is a reduction in force due to applied suction on the entire penetration
393 depth in each of the tests, all in range of 40-60%.

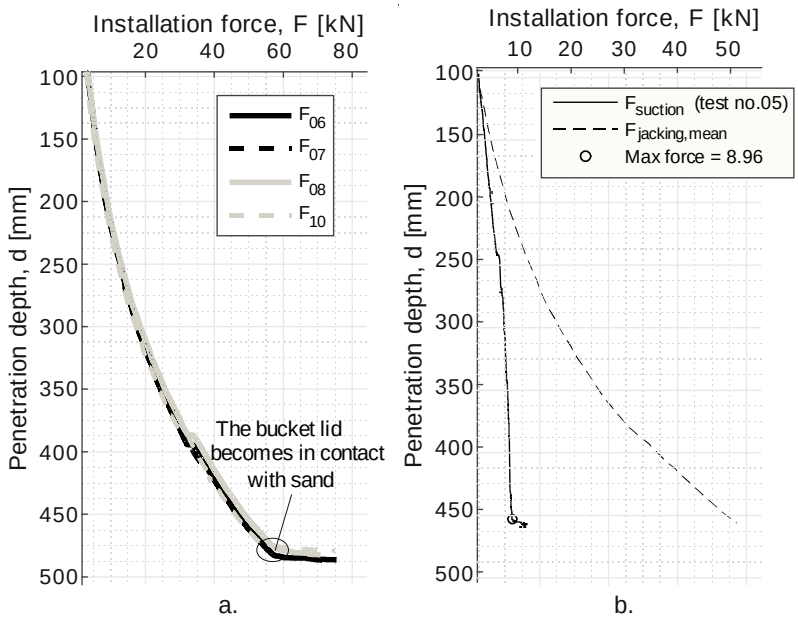

394

395 **Figure 7.** Results of installation tests

396 When comparing the maximum required value of force from the suction installation tests (Table 2)
397 with a mean maximum value of force from all 4 jacking installation tests (57kN), the reduction in
398 this number is between 79.7 – 84.4 %.

399 The reduction in force can only be explained by the reduction of soil penetration resistance. Results
400 can be compared with the past researches, where by analyzing results of applied force, the
401 reduction factor for soil penetration resistance was found. Allersma et al. (2003) mentioned the
402 reduction factor of 8, which was found from centrifuge installation tests. Lian et al. (2004) found a
403 reduction of 78 – 94% while comparing the suction installation with the jacking installation on 1G
404 set-up with a small-scale model. The results are comparable with the findings described above.

405 ***Soil heave development***

406 The sand loosening is beneficial for the installation because it reduces the penetration resistance.
407 However, at the same time, the sand loosening is also responsible for the appearance of sand heave

408 inside the bucket. It has already been proven by previous experimental studies in dense sand that
409 the inside heave of soil is highly probable for the suction installation process (Allersam et al 2003,
410 Tran et al. 2005). The appearance of heave might be problematic for the further in-place bucket
411 performance as it can result in a lower total stiffness of the foundation. Therefore, the development
412 of heave must be taken into consideration during the design. Table 4 shows the height of heave
413 development during all tests. The suction installation results in slightly larger heave than the jacking
414 installation.

415 The reason why the soil moves towards the bucket cavity during the installation in sand is dictated
416 by the volume expansion. Firstly, the volume expansion is a result of the change in the void ratio.
417 The change in void ratio is also given in Table 4. The increase in void ratio for inside plug results in a
418 larger volume of voids. With constant volume of solid material, the increase in total volume results
419 in heave increase. Additionally, soil that is replaced by the bucket skirt is pushed either inside or
420 outside of the bucket. However, the generated flow during the suction installation pushes the soil
421 rather inside together with the direction of the flow. The height of heave is given as a percentage of
422 the total skirt length, r_{heave}. For the suction installation tests the value ranges from 8.4% to 11.4%.
423 For the jacking installation tests the value ranges between 6.6% and 8.0%. Tran et al. (2005)
424 mentioned 6-8% of embedded length as a heave development for suction installation tests. Allersma
425 et al. (2003) observed similar results, where soil heave is described to be dependable on the wall
426 thickness, giving the increase of 5 to 10%. In the laboratory set-up presented in this paper the
427 influence of wall thickness of bucket foundation was not tested. However, the results of heave
428 development are in comparable range with results found in literature. The average value of heave
429 development for suction installation tests is 9.5%. The difference between the jacking tests and the
430 suction tests is expected to be even more significant for the full-scale tests.

Skirt-soil interaction due to seepage

The seepage flow around the bucket skirt is an expected effect of the applied suction as already discussed in the paper. The recorded pore pressures, $p_{measured}$, accompanied with calculated excess pore pressures, u, for test no.05 are given in Fig. 8a. and b. respectively. Results show the variation of pore pressures during suction installation. The result of pore pressure is recorded directly from the laboratory showing the total pressure that the soil experiences at given time. This means that the records show the hydrostatic pressure from the water and the excess pore pressure cumulated during the installation. In order to obtain the excess pore pressure a hydrostatic pressure is subtracted from its total value of pressure.

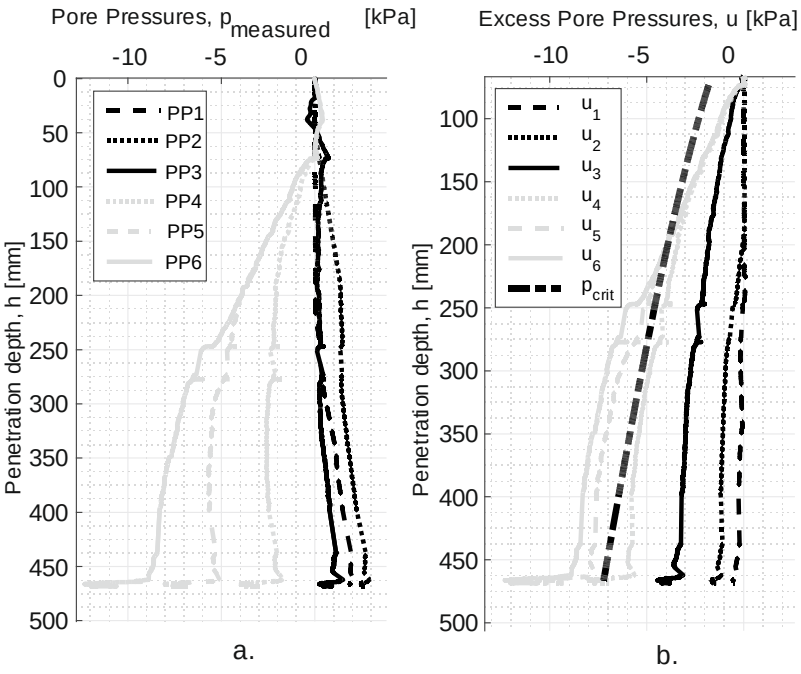

Figure 8. Pore pressure results of the suction installation for test no.05: measured pore pressure (a.) and calculated excess pore pressure (b.)

PP6 shows the suction pressure applied during the installation under the bucket lid. Note that the excess pore pressure refereed as u_6 is and exact value of the applied pressure, p. The rest of

445 transducers show a total pressure including both the hydrostatic pressure and the excess pore
446 pressure. There is a significant amount of excess pore pressure on the inside of the skirt (PP4 and
447 PP5). The measured pressure is already negative, even though the hydrostatic pressure has not yet
448 been deducted (Fig.8a.). On the outside skirt the excess pore pressure is much smaller (PP1-PP2),
449 and after extracting the hydrostatic value from the measured pressure, the values become closer
450 to zero. It can be clearly seen that approaching the skirt tip from the outside soil surface and next
451 the inside plug of the bucket, there is an increase in generated excess pore pressure. The seepage
452 flow is induced because of the difference in hydraulic head: water flows from a higher energy to a
453 lower energy. The seepage produces the excess pore pressure. According to results of excess pore
454 pressure there is an upward flow on the inside wall of the bucket and the soil penetration
455 resistance is reduced by reduction in the effective stress. The downward flow on the outside skirt
456 is limited only to the part close to the skirt tip, as it can be seen that there is almost no excess pore
457 pressure at location PP1. The seepage flow is limited , thus the changes in excess pore pressure at
458 the outside skirt are less significant in comparison to the changes at the inside skirt. Therefore, it is
459 reasonable to assume a constant soil penetration resistance on the outside skirt and a reduction in
460 the inside soil plug.

461 Interestingly, the suction applied during all of the installation exceeds the value of the theoretical
462 critical suction given by Koteras et al (2016), see Eqs.(8 and 11). However, during suction installation
463 tests no piping failure occurred. The exceedance of critical suction pressure is shown in Fig. 8b. The
464 piping is assumed to be formed around the skirt tip and proceed upper to the inside soil surface.
465 While reaching the soil surface a hydraulic seal between the soil and the skirt is broken and a failure
466 occurs. In such a case no further installation is possible. All of tests performed in the laboratory were

fully accomplished. The discussion on the exceedance of critical pressure is presented later on in the paper.

Fig. 9a. and b. shows the changes in pore pressure during the jacking installation on the example of test no.06.

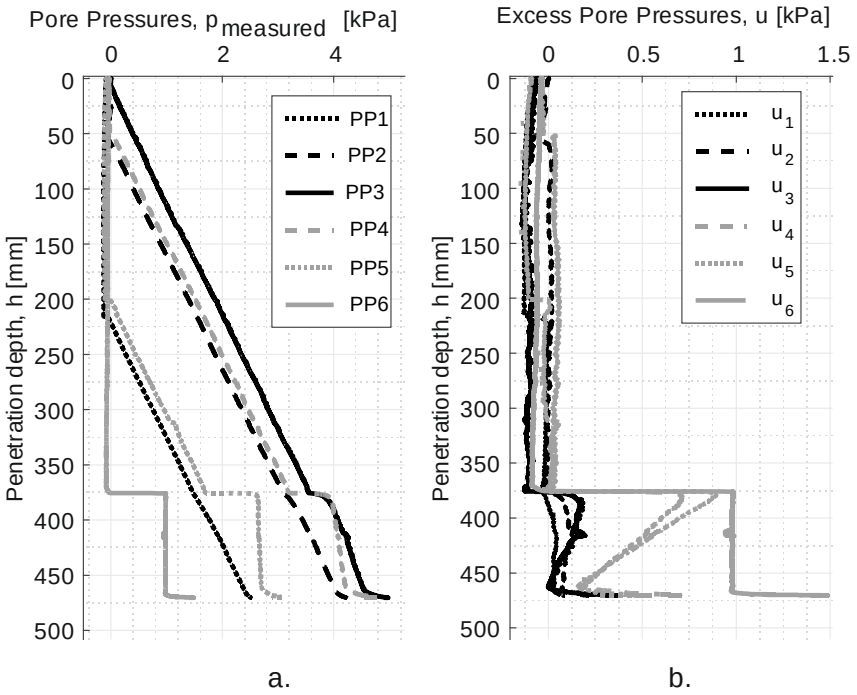

Figure 9. Pore pressure results of the jacking installation for test no. 6: measured pore pressure (a.) and calculated excess pore pressure (b.)

There is no development of the excess pore pressure during the jacking installation, so no seepage flow is expected. The change of 1 kPa for the last stage of installation is observed for all jacking installation tests and it is related to the height of valves on the bucket lid. These valves are open during force installation and from the time when the bucket lid becomes in the contact with water, the water column inside the valves raises up to the level of its height resulting in a 1 kPa change

during the last step of the jacking installation tests. As the seepage flow is not developed, there are no significant changes in soil penetration resistance.

To support the statement that there is a reduction in soil penetration resistance, the average hydraulic gradients have been calculated based on the results of excess pore pressure. The gradient was calculated in 5 different locations, see Fig.10, based on results of excess pore pressure in locations PP1 –PP6 and based on the distance between the reading points.

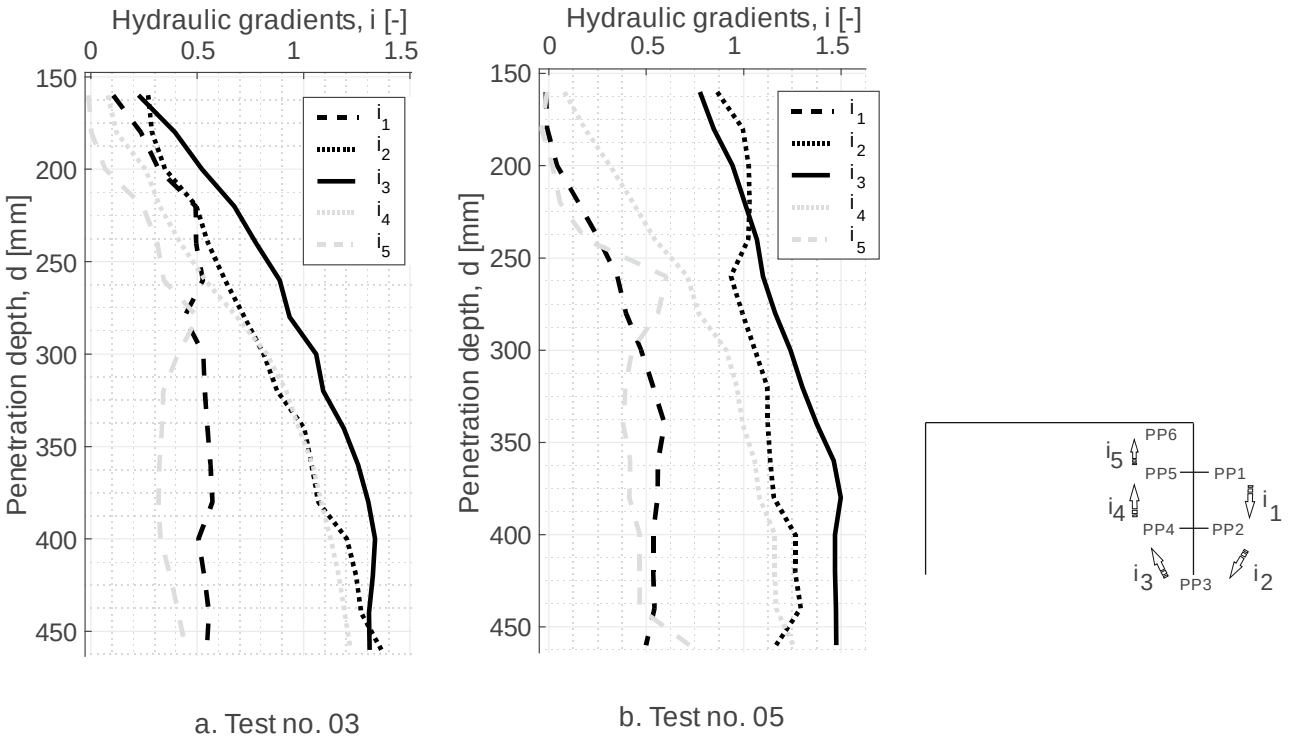

Figure 10. Calculated hydraulic gradients around the skirt during suction installation

As expected, there is the highest gradient around the skirt tip, thus the highest reduction in soil resistance is expected in this location. There are high gradients close to the tip on both, inside and outside skirt. Nevertheless, it is assumed that the high gradient on the outside is probably resulting from a big excess pore pressure changes but only in a close vicinity of the tip. It should be noted

491 that only 6 reading points are available, so the gradients are only roughly approximated. Two
492 calculated gradients closest to the soil surface inside and outside the bucket are small, with a value
493 of around 0.5, what confirms that there was no piping failure during the installation. Interestingly,
494 those gradients become stable at the very early stage of the installation even though the applied
495 suction was still increasing. It can be concluded that the applied suction was within the limits, even
496 though the theoretical limit was exceeded.

497 The reduction is however dependable on the amount of applied suction. The reduction ratio is
498 calculated as a ratio between the suction installation force, $F_{suction}$, and the average values of force
499 from all 4 jacking installation tests, $F_{jacking,mean}$. Fig.11 presents this ratio versus the ratio of
500 pressures: the applied pressure normalized by the theoretical critical suction pressure (Koteras et
501 al. 2016).

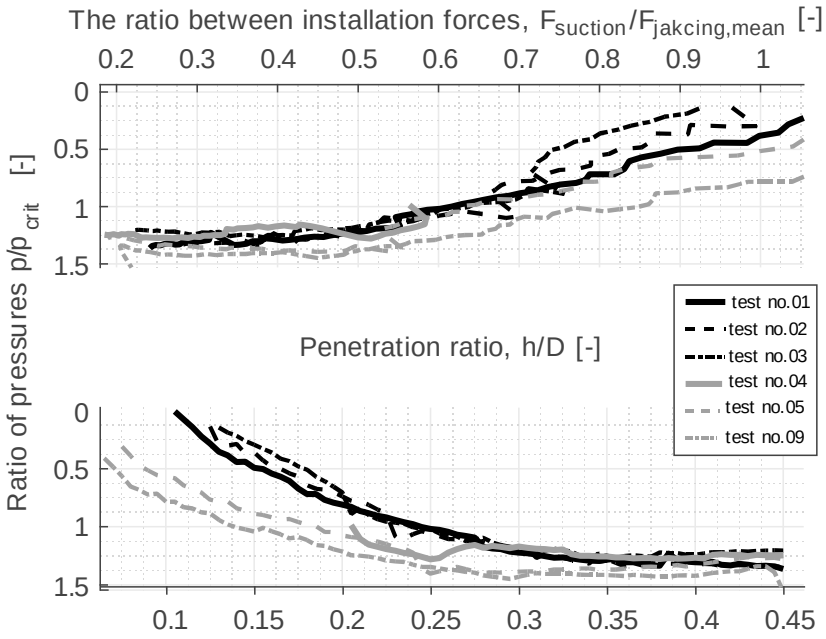

502

503 **Figure 11.** Resistance ratio between suction and jacking installations

Clearly, a reduction in soil resistance takes place due to the seepage flow induced by the applied suction under the bucket lid. When the value of applied pressure increases so does the reduction. The reduction factor higher that 1 at the beginning of the installation should be ignored. The lower graph in Fig. 11 implicates that the ratio of pressure reaches value close to 1 at the very early stage of the installation. In this stage, the force applied for the jacking installation was smaller than the force resulting from the self-weight of the bucket. As the suction force includes both, the force arising from applied suction and the self-weight of the bucket, the reduction ratio is bigger than 1 in this early stage.

It can be also observed that in the early stage of the installation there is a slightly smaller reduction in the first three tests (test no.01-03) and this is due to bigger self-load applied to the installation. As the self-penetration was longer, the suction was applied a bit later. However, when the penetration proceeds and gets to its final stage, there are no visible differences in the reduction and in the final required force. The values of required suction at the penetration depth h=450 mm are given in Table 2.

Finally, again the exceedance of the theoretical critical suction can be observed based on Fig.11. Interestingly, there is a stabilization of suction when the pressure ratio is around 1.3. This might suggest that the allowable suction lies in this range.

Boundary effects

The accuracy of scaled tests in laboratory often depends on the boundary conditions that the set-up applies for. The seabed is rather unlimited, whereas the set-up boundaries are situated in a close vicinity of testing area. During each of the installation tests, the beam with pore pressure transducers is inserted into the soil at the closest possible distance to the wall of soil container, see

526 Fig. 2. The positions of the pore pressure transducers on the beam are indicated in Fig. 12a. Those
527 transducers are zeroed before the start of each test, so the direct measurements indicate the value
528 of excess pore pressure. As an example, the excess pore pressures developed in the localization of
529 the beam versus the penetration depth for the bucket during the test no.5 is given in Fig. 12b. This
530 test is a suction installation test and the significant development of a negative pore pressure is
531 observed, increasing together with the progression of the installation. The same trend happens to
532 all suction installation tests, whereas for jacking installation tests changes of the pore pressure at
533 the boundary are negligible.

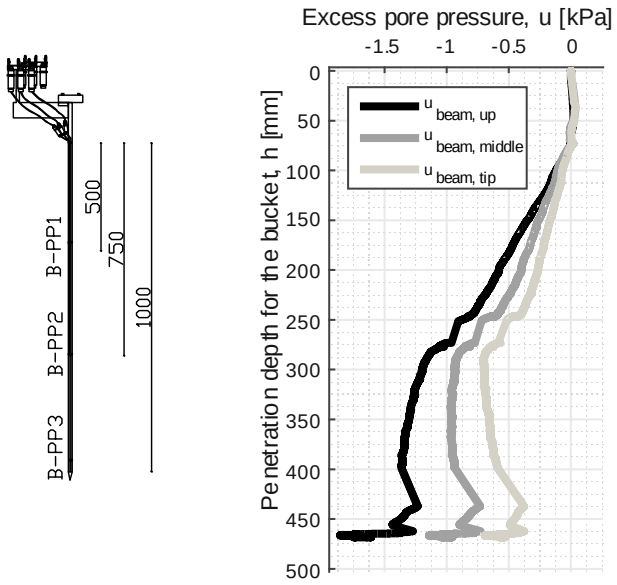

534

535 **Figure 12.** Beam with pore pressure transducer (a.) and results of excess pore pressure at the
536 beam during the suction installation (b.)

537 The presence of the excess pore pressure at the boundaries is the reason why the theoretical critical
538 suction should be accounted in the numerical calculations of the seepage flow around the bucket.
539 If there is a seepage flow present at the boundaries, it has an influence on the seepage flow around

the bucket skirt. The model should include the same boundary conditions as the laboratory model, so that the comparison is reasonable. This has been examined and it is described in the following section.

Comparison of the results for excess pore pressures and the applied suction

The results of numerical simulations are compared with mean values of excess pore pressure from test no.05 and 09. The numerical simulations of installation provides also only results of total pore pressure that soil experience and the values of excess pore pressure are calculated by extracting the hydrostatic pressure. Figure 13 presents the development of excess pore pressure due to applied suction from both, laboratory tests and numerical simulations.

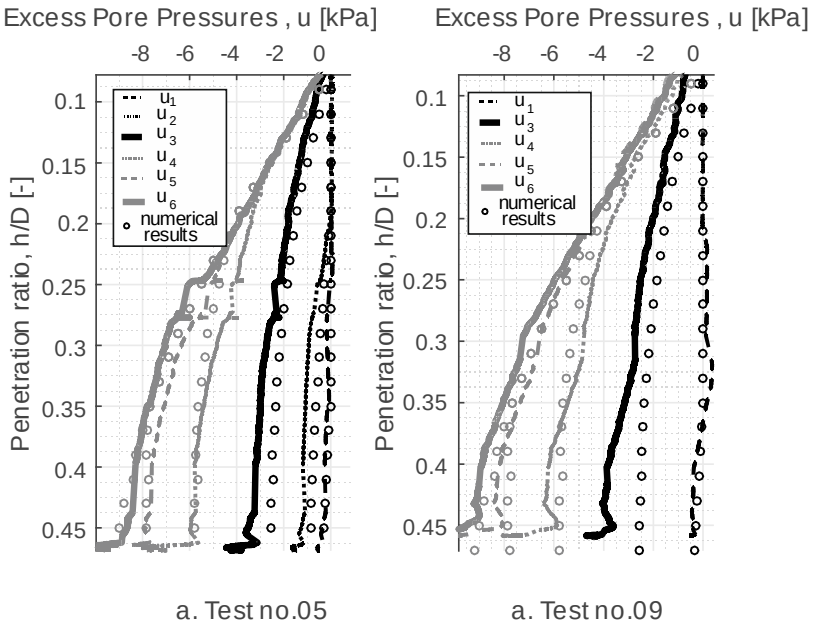

Figure 13. Comparison of the change in pore pressures at the skirt between numerical results and laboratory results

The results of excess pore pressure are comparable what confirms that the numerical model works correctly. The trend for the development around the skirt is the same for both, numerical and

laboratory results. Most of the data is well fitted and the numerical model reflects results of the laboratory installation tests (the accuracy of the pressure transducers used in the laboratory tests is ±0.2 kPa). Results are the most differing for the skirt tip. The change between the numerical model and results from the installation tests is around 1kPa. More excess pore pressure is measured during the laboratory test that it is predicted with the numerical simulations. The numerical simulations, however, are performed for the stationary flow. In general, the suction installation of the bucket foundation is assumed to be stationary. Nevertheless, the most of the flow develops around the bucket tip and, as the bucket is constantly penetrated into the soil, the seepage has no time to be fully developed. If assuming that the stationary seepage is not fully developed, the flow behavior around the tip might differ from the numerical results.

The boundary effects influence the formulation of pore pressure factor (the ratio of the excess pore pressure at the skirt tip to the applied suction). It can be seen based on the laboratory results that there is a development of excess pore pressure in the vicinity of sand container walls. Therefore, it is assumed that the seepage flow is somehow changed and so thus the development of the excess pore pressure around the skirt. Eq.(15) is a new formulation for the pore pressure factor.

$$\alpha_{\mathrm{new}} = 0.47 - 0.25\left(1 - exp\left(-\frac{\mathrm{h}}{\mathrm{D}\cdot 0.32}\right)\right) \tag{15}$$

The observation of the excess pore pressure around the tip from the numerical simulations is however showing an increase in this value in relation to the laboratory results. Fig.14 presents the new formulation of pore pressure factor as a function of penetration ratio, $\left(\frac{h}{D}\right)$. Next to the formulation, the results of pore pressure factor from laboratory test no.05 and no.09 are plotted.

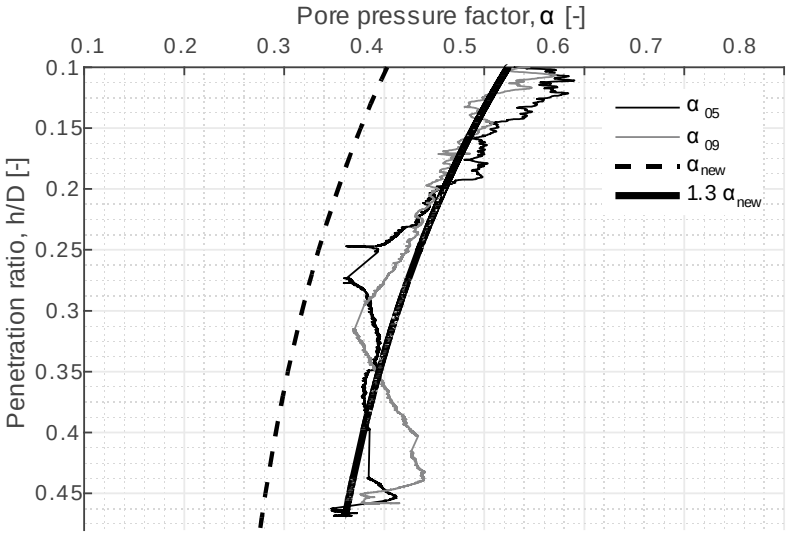

574

575 ***Figure 14.*** *Pressure factor at the tip: comparison of numerical results with laboratory tests*

576 It has been noted that when comparing these results, there is an increase in the pore pressure ratio
577 of around 30% for the laboratory results, even though the numerical model has been accounted for
578 new closed boundary conditions. As mentioned before the seepage flow is the highest at this point
579 and probably goes beyond the stationary flow. The increased value of new fitted function for pore
580 pressure factor seems to fit the results of laboratory tests. It is not however recommended to
581 increase this value for the design. This is an observation based on the presented laboratory results
582 and it requires further investigation.

583 The pore pressure factor can be used for the design of the reduced soil penetration resistance
584 throughout the calculation of approximated gradient around the skirt. However, it is still unclear
585 why the pressure applied during the installation can and often exceeds the theoretical value of
586 critical suction with no effects of piping. The critical condition for the stationary flow arises when
587 critical gradient is developed: $i = i_{crit} = \gamma'/\gamma_w$. The consideration of γ' is therefore important and
588 the higher value for sand allows for more suction before reaching the critical gradient as it will be

now increased. The increase of $\gamma'$to 14 kN/m^3 leads to better estimation where the applied suction fits in the limits, however, such a value gives unrealistic values of in-situ void ratio for sand, which is not in the range given by the maximum and the minimum void ratio. This estimation is shown in Fig. 15. As it cannot be increase in γ' that results in higher critical suction, then it should be the seepage length ($p_{crit} = s \cdot \gamma'$). The seepage length is dependable on the exit hydraulic gradient (eq. 6), and the gradient can be calculated from Darcy's law as a ratio of the flow velocity at the exit, v_{exit}, and the hydraulic conductivity, k. As the previous sections indicates that there is a loosening of soil plug it seems reasonable to investigate the hydraulic conductivity of soil, as it does have a great influence on the value of critical suction. An increase in hydraulic conductivity is followed by a decrease in exit hydraulic gradient and next by an increase in the seepage length. Based on the results of laboratory installations and CPTs performed before and after suction installation, increased value of k is used for the inside soil plug when calculating the critical pressure ($k = 1 \cdot 10^{-4}$ m/s is used). This resulted in a new formulation for the normalized seepage length, eq.(16). The critical suction pressure based on the normalized seepage length from eq.(16) is included in Fig.15.

$$\left(\frac{\mathrm{s}}{\mathrm{h}}\right)_{\mathrm{exit,new}} = 1.25 \cdot \left(\pi - atan\left[2.5\left(\frac{\mathrm{h}}{\mathrm{D}}\right)^{0.74}\right]\left(2 - \frac{1.8}{\pi}\right)\right) \quad (16)$$

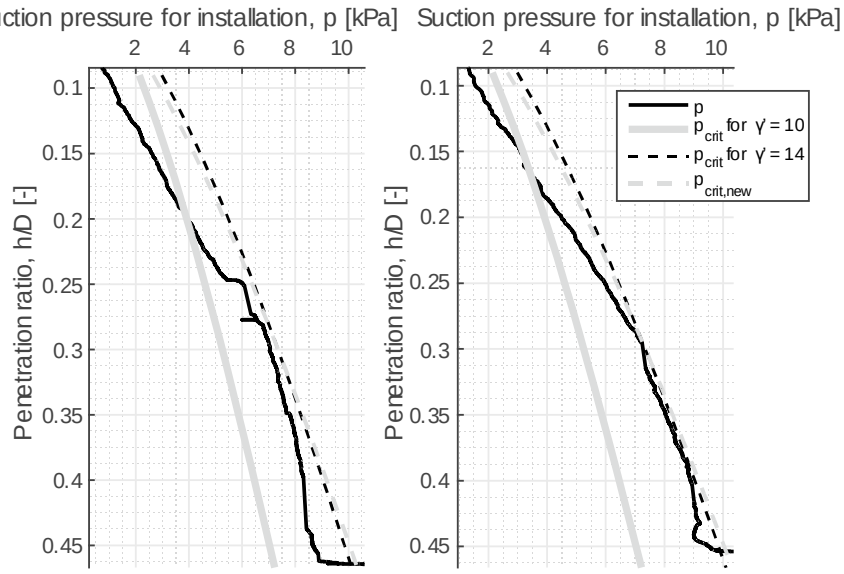

605

606 **Figure 15.** Comparison of applied suction with critical values based on numerical simulations

607 It is concluded that the hydraulic conductivity for the inside soil plug is increased, and therefore,
608 more suction can be applied without causing a piping problems. With a high probability, the same
609 trend should be applied with the full-scale tests, however, it requires a confirmation. The ratio
610 between initial hydraulic conductivity and the increased value for the inside plug, k_{out}/k_{in}, is equal
611 to 1.4. Similar observation has been made by Tran et al. (2005). The results of centrifuge tests on
612 the installation of bucket foundation have shown that for increasing penetration the soil relative
613 density drops, hence the sand becomes looser. The ratio between soil hydraulic conductivities is in
614 a range between 1 to 2 with an average value of 1.5.

615 **Conclusions**

616 A soil-skirt interaction during suction and jacking installation of the bucket foundation has been
617 analyzed by performing 10 medium-scale tests in the dense sand. The comparison between soil
618 resistance during two different installations indicates a significant reduction in favor for the suction

619 installation. The reduction is also confirmed by measuring soil conditions before and after each
620 installation through CPT-s. The comparison of calculated soil relative density indicates a major
621 decrease in sand density for the inside plug, however, the changes on the outside of the bucket are
622 negligible. This confirms the proposed assumptions for the calculation of penetration resistance
623 during the suction installation. Whereas the inside friction and the tip resistance is reduced by the
624 applied suction, the possible increase on the outside friction can be neglected.

625 Measured results of excess pore pressure around the bucket skirt during the suction installation
626 confirm the appearance of seepage flow that in general reduces the soil penetration resistance.
627 Results of gradients developed during the installation are helpful in the assessment of redistribution
628 of effective stresses, thus the changes in soil penetration resistance. Additionally, the reasonable
629 comparison of the test measurements with the results of numerical simulations validates the FE
630 model and its assumptions. This allows for better understanding of the limits for the critical suction
631 against the piping. The sand loosening within the inside plug results in an increase of the hydraulic
632 conductivity. Assuming that the stationary seepage flow is not fully developed when the bucket
633 penetrates into the soil allows to use an increased hydraulic conductivity in calculation of theoretical
634 critical suction. The stationary flow calculation gives a lower limit for the suction. An increase
635 hydraulic conductivity increases this limit what is beneficial for the suction installation. This will
636 allow deeper suction installation and the installation of larger buckets.

637 The last but not least, the heave development for the suction installation in dense sand is observed
638 in all of the tests, giving the heave height of around 10% of total skirt length. The inside soil heave
639 must be included in the design, as it can decrease the total stiffness of the foundation.

Acknowledgements

The research is funded by "EUDP Project" and by EU7 as a part of the Project "INNWIND - Innovative Wind Conversion Systems (10-20 MW) for Offshore Applications". The support is greatly appreciated.

References:

Allersma, H.G., Plenevaux, F., and Wintgens, J. 2003. Centrifuge research on suction piles: installation and bearing capacity. In Proceedings of BGA International Conference on Foundations: Innovations, observations, design and practice, Dunndee, UK, pp. 91-98.

Andersen, K. H., Jostad, H. P., and Dyvik, R. 2008. Penetration Resistance of Offshore Skirted Foundations and Anchors in Dense Sand. Journal of Geotechnical and Geoenvironmental Engineering, 134(1): 106-116.

API. 2014. Recommended practice for planning, designing and constructing fixed offshore platforms – Working stress design. American Petroleum Institute: Recommended practise 2A-WSD, Washington, D.C., 22nd Edition.

Chen, F., Lian, J., Wang, H., Liu, F., Wang, H., and Zhao, Y. 2016. Large-scale experimental investigation of the installation of suction caissons in silt sand. Journal of Applied Ocean Research, 60: 109-120.

DNV. 1992. Foundations, classification notes No. 30.4. Det Norske Veritas, Høvik, Norway, 134th Edition.

Erbrich, C., and Tjelta, T. 1999. Installation of bucket foundations and suction caissons in sand – Geotechnical performance. In Proceedings of 31st Annual Offshore Technical Conference, Houston, Texas, OTC 10990(1): 725-736.

Harireche, O., Mehravar, M., and Alani, A. 2014. Soil condition and bounds to suction during the installation of caisson foundations in sand. Journal of Ocean Enineering, 88: 164-173.

Houlsby, G. T., and Byrne, B. W. 2005. Design procedure for installation of suction caissons in sand. Journal of Geotechnical Engineering, 158(3): 135-144.

Ibsen, L. B. 2008. Implementation of a new foundations concept for offshore wind farms. In Proceedings of Nordisk Geoteknikermøte Nr. 15: NGM 2008, Sandefjord, Norway, pp. 19-33.

Ibsen, L.B., and Brødker, L. 1994. Baskarp Sand no. 15: data report 9301. Data Report 9401. Aalborg University, Aalborg.

Ibsen, L. B., and Thilsted, C. 2011. Numerical Study of Piping Limits for Suction Installation of Offshore Skirted Foundations and Anchors in Layered Sand. In Proceedings of International Symposium on Frontiers in Offshore Geotechnics (ISFOG), Perth, Australia, pp. 421-426.

Ibsen, L. B., Hanson, M., Hjort, T., and Thaarup, M. 2009. MC-Parameter Calibration of Baskarp Sand No. 15. DCE Technical Report, No. 62, Aalborg University, Denmark.

Koteras, A. K. 2017. Set-up and Test Procedure for Suction Installation and Uninstallation of Bucket Foundation. DCE Technical Memorandum, No. 63, Aalborg University, Denmark.

Koteras, A. K., Ibsen, L. B., and Clausen, J. 2016. Seepage Study for Suction Installation of Bucket Foundation in Different Soil Combinations. In Proceedings of 26th International Ocean and Polar Engineering Conference, Rhodos, Greece, 26 June-2 July, pp. 697-704.

Lehane, B., Schneider, J., and Xu, X. 2005. The UWA-05 method for prediction of axial capacity of driven piles in sand. In Proceedings of International Symposium on Frontiers in Offshore Geotechnics (ISFOG), Perth, Australia, pp. 19-21.

Lian, J., Chen, F., and Wang, H. 2004. Laboratory tests on soil-skirt interaction and penetration resistance of suction caissons during installation in sand. Journal of Ocean Engineering, 84: 1-13.

Senders, M., and Randolph, M. F. 2009. CPT-based method for the installation of suction caissons in sand. Journal of Geotechnical and Geoenvironmental Engineering, 135(1): 14-25.

Sjelmo, A. 2012. Soil-Structure Interaction in Cohesionless Soils during Monotonic Loading. Student thesis: Master thesis, Aalborg University, Denmark.

Tjelta, T. 1995. Geotechnical experience from the installation of the Europipe jacket with bucket foundations. In Proceedings of 27th Annual Offshore Technical Conference, Houston, Texas, 2: 897-908.

Tran, M., and Randolph, M. 2008. Variation of suction pressure during caisson installation in sandinstallation of caisson foundations in sand. Journal of Geotechnique, 58(1): 1-11.

Tran, M., Randolph, M., and Airey, D. 2005. Study on seepage flow and sand plug loosening in installation of suction caissons in sand. In Proceedings of 15th International Offshore and Polar Engineering Conference, Seoul, Korea, 19-24 June 2005, pp. 516-521.

Vaitkunaite, E., Ibsen, L. B., and Nielsen, B. 2014. New Medium-Scale Laboratory Testing of Bucket Foundation Capacity in Sand. In Proceedings of 24th International Offshore and Polar Engineering Conference, Busan, Korea, pp. 514-520.

Table 1. Range of values for soil parameters from CPT for all installation tests

Soil parameters	Range of values
Relative soil density [%]	88 - 91
Triaxial friction angle [°]	54 - 54.5
Triaxial dilation angle [°]	19.9 - 20.5
In situ void ratio [-]	0.625 - 0.653
Effective soil unit weight [kN/m^3]	9.7 - 9.9

Table 2. Overview of test campaign

Test no.	Driving force for the installation	Maximum installation force, F_{max} [kN]	Required suction for $h = 450$mm, p_{req}[kPa]	Self-weight penetration, $h_{self\text{-}weight}$ [mm]	Maximum penetration, h_{max} [mm]
01	Suction + Force	11.56	9.18	125	462/ 470
02	Suction + Force	11.58	9.21	127	468 / 468
03	Suction + Force	11.05	8.23	130	468 / 471
04	Suction	8.92	8.53	78	460 / 474
05	Suction	8.96	8.67	73	462 / 466
06	Force	57.7	-	-	483 / 487
07	Force	59.1	-	-	483 / 488
08	Force	58.01	-	-	477 / 482
09	Suction	9.65	9.52	66	447 / 458
10	Force	53.1	-	-	472 / 479

Table 3. Results of relative soil density, I_D, and results of effective soil unit weight, γ'

Test no.	Before installation		After installation			
			Inside the bucket		Outside the bucket	
	$I_{D,mean}$ [%]	γ'_{mean} [kN/m^3]	$I_{D,mean}$ [%]	$\Delta I_{D,mean}$ [%]	$I_{D,mean}$ [%]	$\Delta I_{D,mean}$ [%]
01	87.83	9.73	62.99	28.28	74.69	14.96
02	90.78	9.88	65.65	27.68	75.61	16.71
03	88.78	9.78	64.11	27.79	85.83	3.32
04	91.13	9.90	66.33	27.21	82.33	9.66
05	90.30	9.86	66.69	26.15	85.05	5.81
06	89.12	9.80	87.19	2.16	85.48	4.08
07	88.72	9.78	85.38	3.76	82.88	6.58
08	90.59	9.88	85.53	5.59	82.54	8.20
09	90.29	9.86	63.76	29.38	82.89	8.20
10	89.74	9.83	85.78	4.41	83.78	6.64

Table 4. The change in void ratio and corresponding height of inside heave

Test no.	Height of heave plug, h_{heave}[mm] (±5)	Void ratio before, e_{before}[-]	Void ratio after, e_{after} [-]	Ratio of heave height to the skirt length, r_{heave} [%]
01	45	0.653	0.867	9.0
02	47	0.628	0.844	9.4
03	44	0.645	0.857	8.8
04	42	0.625	0.838	8.4
05	49	0.632	0.835	9.8
06	38	0.637	0.659	7.6
07	40	0.646	0.674	8.0
08	33	0.630	0.673	6.6
09	57	0.632	0.860	11.4
10	36	0.637	0.671	7.2

List of figures

1. Installation of the bucket model in the sand container
2. Laboratory set-up (dimensions in mm)
3. Model of bucket foundation (dimensions in mm)
4. Positions for CPTs before (a.) and after installation test (b.) (dimensions in mm)
5. Meshed numerical model with boundary conditions (dimensions in mm)
6. Comparison of relative soil density before and after installation: test no.05 (a. and b.) and test no.06 (c.); see Fig. 4 for locations of CPTs
7. Results of installation tests
8. Pore pressure results of the suction installation for test no.05: measured pore pressure (a.) and calculated excess pore pressure (b.)
9. Pore pressure results of the jacking installation for test no. 6: measured pore pressure (a.) and calculated excess pore pressure (b.)
10. Calculated hydraulic gradients around the skirt during suction installation
11. Resistance ratio between suction and jacking installations
12. Beam with pore pressure transducer (a.) and results of excess pore pressure at the beam during the suction installation (b.)
13. Comparison of the change in pore pressures at the skirt between numerical results and laboratory results
14. Pressure factor at the tip: comparison of numerical results with laboratory tests
15. Comparison of applied suction with critical values based on numerical simulations